International Journal of Adhesion & Adhesives 67 (2016) 3–13

Contents lists available at ScienceDirect

International Journal of Adhesion & Adhesives

journal homepage: www.elsevier.com/locate/ijadhadh

Evaluation of the height 3D roughness parameters of concrete substrate and the adhesion to epoxy resin

Ł. Sadowski *, S. Czarnecki, J. Hoła

Faculty of Civil Engineering, Wroclaw University of Technology, Wybrzeze Wyspianskiego 27, 50-30 Wroclaw, Poland

ARTICLE INFO

Available online 30 December 2015

Keywords:
Concrete
Surface morphology
Adhesion
Interfaces

ABSTRACT

In this work a newly designed three-dimensional (3D) scanner was used in order to evaluate and describe the morphology of selected concrete substrate surfaces. A special focus was placed on the advantages and disadvantages of the latter over the other scanners. The interseting results of such an investigation for 3 differently treated existing concrete substrates are selected and presented. It was found that with an increase of maximum aggregate grain size in concrete, the values of arithmetical mean height (*Sa*), the root mean square height (*Sq*) and skewness (*Ssk*) for the shotblasted surface also increase, while the value of the kurtosis (*Sku*) grows for ground surfaces and decreases for the shotblasted surface. It was also found that there is a relation between the values of height parameters *Sku* and the maximum height of peaks (*Sp*) with the pull-off adhesion (f_b) of the epoxy resin added layer and these surfaces.

1. Introduction

Nowadays in housing, epoxy resins are more often used as an added layer on concrete substrates in concrete floors [1]. These substrates are usually made using low-strength concrete with a compressive strength of between 10 and 15 MPa and a maximum size of aggregate grain in the concrete of 2, 4 or 8 mm. Before placing the added concrete layer, the surface of the substrate can usually be specially treated using grinding, sandblasting, shotblasting or milling [2,3]. However, for economic reasons the final concrete surfaces are finished by patch grabbing, and only in specific cases are treated using special surface treatment methods. The surface treatment method has an influence on the morphology of the concrete substrate and therefore on the pull-off adhesion between the concrete substrate and the epoxy resin added layer.

In the last few years, three-dimensional (3D) methods are more often applied for the measurement of concrete morphology metrology. Currently, height parameters have started to be used to evaluate the surface morphology of concrete elements. There is a lack of knowledge in literature regarding these kind of applications. Therefore, the purpose of this article, among others, is the extension of knowledge in this area.

Hence, a comprehensive overview of the methods of surface morphology analysis in a 3D context, which includes a 3D scanner that was constructed for the purpose of the concrete surface study, is described in the article. The results of the analysis of height parameter values, which were obtained with the use of this scanner and which describe the morphology of nine differently treated surfaces of elements made of concrete with different maximum aggregate grain size, are presented. The paper is also enriched with research which enables a relation between the height parameters and the pull-off adhesion of these surfaces to the epoxy resin added layer to be assessed.

2. Literature survey

It is worth beginning by recalling that the first studies regarding the research of surface morphology in a two-dimensional (2D) context date back to the beginning of the 30's of the XX century [4]. The first standard, prepared by the International Organization for Standardization (ISO), which related to such studies was published in 1966 [5], while the first international conference on this issue was held in 1968. The result of a measurement of 2D methods is shown as a roughness profile in Fig. 1a [6].

The concrete surfaces were usually measured using 2D roughness parameters such as arithmetical mean deviation (*Ra*) and the maximum height of profile (*Rz*) [7]. Analyses made by Courard [8–11] presented that the roughness of the concrete substrate is a common

* Corresponding author.
E-mail addresses: lukasz.sadowski@pwr.edu.pl (Ł. Sadowski), slawomir.czarnecki@pwr.edu.pl (S. Czarnecki), jerzy.hola@pwr.edu.pl (J. Hoła).

http://dx.doi.org/10.1016/j.ijadhadh.2015.12.019
0143-7496/

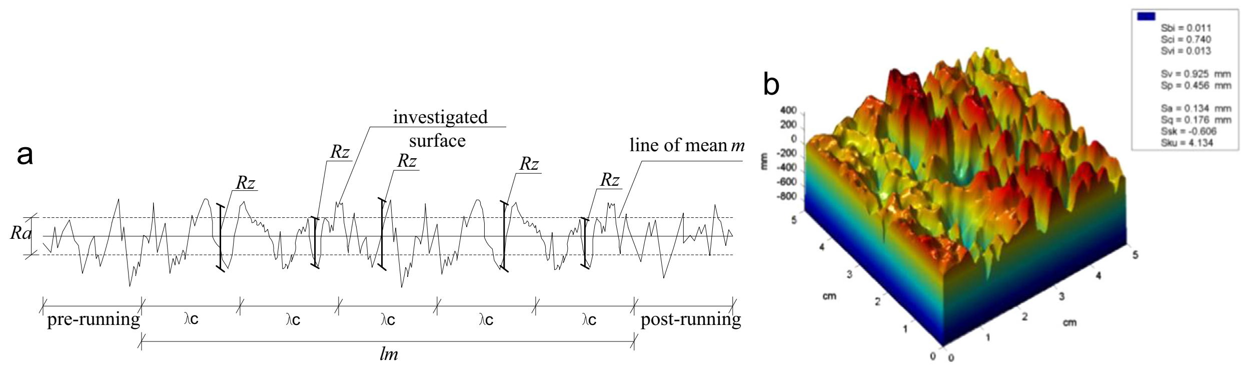

Fig.1. Exemplary: (a) roughness profile of a surface described by 2D parameters, and (b) 3D isometric view of a surface with 3D roughness parameters which describe it.

factor influencing adhesion. Franck and De Belie [12] found the relation between concrete surface roughness (measured by *Ra* and *Rz*) and contact pressures between floor and bovine claw. Santos and Julio [13] presented the correlation between 2D roughness parameters and bond strength with the use of a specifically developed laser roughness analyser [14]. Siewczyńska [15] presented the influence of the ratio of a rough surface to its projection on a plane (R_S) on pull-off adhesion. Garbacz et al. [16] also found correlations between the concrete surface roughness parameters and the adhesion. Maerz et al. [17] studied the bond behaviour between the concrete and epoxy using laser striping and image analysis.

As mentioned in [18–20] there is an influence of surface roughness parameters on adhesion and it depends on the type and grading of the aggregate and the compressive strength of the existing concrete substrate. The studies presented in [21–25] show that a higher bond strength is achieved by increasing the surface roughness through surface treatment for high-strength concretes. Courard et al. [26] stated that selection of a suitable surface treatment technique should be preceded by the analysis of its aggressiveness in relation to the concrete substrate strength. They also stated that if treatment is not well operated with regard to the quality and the strength of concrete it can induce microcracking [26]. Courard et al. [27] stated also that increasing roughness promotes adhesion due to better mechanical interlocking for high-strength concrete substrates and for concrete substrates with compressive strength class lower than C30/37 they recommended less aggressive treatment. There is no study regarding the influence of maximum aggregate grain size in concrete on the surface morphology parameters and pull-off adhesion for low-strength concretes.

The first devices which were used to assess surface morphology in a three-dimensional (3D) context occurred in the 80's of the twentieth century. The finalisation of work on the systematisation of parameters which describe roughness in a 3D context was the study [28] which was released in 1993 and also ISO 25178 [29] standard. According to the adhesion between concrete layers in fib Model Code 2010 [30], three independent effects (cohesion, friction and dowel action) have been proposed. According to Adams and Drinkwater [31] the main types of defects which may occur in multi-layer system are adhesion and cohesion type.

Currently, devices which are used to analyse surface morphology in a 3D context are based on the measurement of point coordinates of the assessed surface [32–37]. On this basis, with the use of specialized computer software, a 3D isometric view of the assessed surface can be generated and on its basis the values of many 3D roughness parameters (Fig. 1b) can be calculated. Six groups of such parameters can be distinguished, namely: height, functional, spatial, hybrid, volume and feature parameters [29,38]. The most commonly used, among the above mentioned parameters, are the parameters of height which are also known as amplitude parameters [28].

In the case of concrete surfaces, when given the choice of 2D methods and 3D surface morphology analysis, 3D methods are considered to be more useful as only they enable geometric features, which are characteristic for concrete surfaces such as: skewness, isotropy, microcracking and the intensity of craters and hills, to be described. The most commonly used methods, with an emphasis on their advantages and disadvantages, were summarised below in Table 1. This information can be useful for researchers who deal with issues regarding the assessment of concrete surface morphology.

From the surface roughness parameters specified in [29], the most commonly used height parameters are listed in Table 2.

Currently, height parameters have started to be used to evaluate the surface morphology of concrete elements. Such an example is the study performed by Ourahmoune et al. [51] who analysed the effect of the surface morphology, described by the *Sa* parameter, created by sandblasting on the wetting and bond strength properties of a neat carbon fibre reinforced matrix and a glass fibre reinforced matrix. Hola et al. [52] critically looked at the possibility of the evaluation of the pull-off adhesion, solely on the basis of the existing concrete surface morphology examinations. Majchrowski et al. [47] stated that the *Ssk* parameter (skewness) can be useful for the evaluation of concrete surfaces. Sadowski [53] showed that the values of the pull-off adhesion of the concrete layers can be identified on the basis of the values of parameter *Sq*. Due to the fact that the height parameters *Sa, Sq, Sp, Sv, Ssk* and *Sku* were provisionally considered as useful for the assessment of concrete surface morphology in previous studies, they were also used in the research presented in this work.

3. Description of the newly designed three-dimensional (3D) scanner

The newly designed 3D scanner based on modification of the linear triangulation method was used and relies on the measurement of the angle between an optical system and a set of laser spots which create a 50 mm long line on the assessed surface. The laser triangulation method is based on light sectioning and determines the position of a light point or line profile observed at a certain angle relative to the direction of light projection [54–56]. As mentioned previously in [52], the larger the angle (α) between the light incidence direction and the observation direction, the higher the sensitivity (s) of the method (Fig. 2). According to [56], the range is calculated as follows:

$$r = B\frac{b_0 \tan\alpha - s}{b_0 + s \tan\alpha} \tag{1}$$

Table 1
The most commonly used 3D methods of surface morphology analysis.

Name and short description of method	Advantages and disadvantages of method in cases of the assessment of concrete surface morphology
Mechanical profilometry [39–40]: Method is based on the measurement of surface roughness with the use of a mechanical contact.	**Advantages:** -High accuracy of measurement,-high speed of measurement. **Disadvantages:** -Mechanical contact of the measuring head with the tested surface which can cause scratches on it and affect the results of research,-lack of mobility,-the need of taking samples for tests from the analysed element,-the possibility of testing samples of a limited height.
Laser profilometry [14, 16]: Method is based on the measurement of surface roughness by using a non-contact optical laser.	**Advantages:** -Non-contact analysis- high accuracy of measurement,-high speed of measurement. **Disadvantages:** -Lack of mobility,-the need of taking samples for tests from the analysed element,-the possibility of testing samples of a limited height.
Vertical scanning interferometry [41–42]: Method enables surface morphology to be analysed with the use of an interferometric microscope.	**Advantages:** -Non-contact surface analysis,- accuracy of measurement,- the possibility to record video during measurement **Disadvantages:** -Lack of mobility,- limited size of the assessed area.
Scanning electron microscopy (SEM) [43–46]: In this method surface morphology analysis is carried out by recording the change in density of a material on the surface of a sample with the use of an electron emission.	**Advantages:** -Non-contact surface analysis,- high accuracy, **Disadvantages:** -Lack of mobility,- the need of taking samples for tests from the analysed element,- limited height of the assessed sample.
Laser scanning [47–48]: Method relies on the measurement of height differences between points located on the assessed surface which is based on deviations of their locations from reference points and is carried out by two cameras simultaneously.	**Advantages:** -Non-contact surface analysis,- high accuracy of measurement,- possibility of analysing large surfaces,- independent measurement carried out simultaneously by two cameras,- mobility, **Disadvantages:** -Necessity to scan a much larger area than the one of interest,- time-consuming calibration in the place of the measurement site,- time-consuming measurement,- three reference points are required in the scanning area.

Table 2
Height parameters which describe surface morphology [based on 28, 29, 49, 50].

Name of parameter	Formula*	Interpretation for the assessment of concrete surface morphology
Arithmetical mean height The root mean square height	$Sa=\frac{1}{A}\int\int_A \lvert Z(x,y)\rvert dxdy$ $Sq=\sqrt{\frac{1}{A}\int\int_A (Z(x,y))^2 dxdy}$	*Sa* and *Sq* parameters are particularly suited to describe the peaks, valleys and spacing of the surface characteristic elements (the spacing of the various texture features).
Skewness	$Ssk=\frac{1}{Sq^3}\frac{1}{A}\int\int_A z^3(x,y)dxdy$	$Ssk>0$ shows the dominance of peaks on the analysed surface, while $Ssk<0$ shows the dominance of valleys. An increase in the *Ssk* value indicates a deterioration of the surface state and an increase of peaks with steep slopes and sharp hills. A negative *Ssk* indicates that the surface is principally composed of one plateau with deep and fine valleys, and a positive *Ssk* indicates a surface with lots of peaks on a plane.
Kurtosis	$Sku=\frac{1}{Sq^4}\frac{1}{A}\int\int_A z^4(x,y)dxdy$	The *Sku* parameter provides information on the probability of defect occurrence and their distribution on the analysed surface. $Sku<3$ indicates a low probability of their occurrence and their regular distribution, whereas $Sku>3$ indicates a high probability of defect occurrence and their irregular distribution.
The maximum height of peaks The maximum height of valleys The maximum height of the surface	$Sp=\sup\{Z(x_i,y_j)\}$ $Sv=\lvert\inf\{Z(x_i,x_j)\}\rvert$ $Sz=Sp-Sv$	*Sp*, *Sv* and *Sz* are parameters calculated on the basis of analysis of the absolute maximum and minimum points located on the analysed surface

* $Z(x, y)$ is the height coordinate within sampling area A.

where b_0 is the distance of the sensor from the optical centre, B is the distance of the light plane from the optical centre and s is the position of the profile on the sensor.

To obtain a field of view width of 50 mm and lateral resolution $Res_X=0.01$ mm, the IVC-3D smart camera was implemented. The camera includes a CMOS sensor with 2048 pixels, red diode laser $\lambda=658$ nm and microcontroller for image segmentation, with a maximum performance of 5000 3D profiles/s. The triangulation angle ($\sigma=53°$) and the surface distance influence vertical resolution, which was set to $Res_Z=0.01$ mm. Longitudinal scanning was done manually using a linear guide integrated with an incremental encoder, ensuring the triggering of individual acquisition with resolution $Res_Y=0.01$ mm. It takes less than 5 s to scan the test surface area of 50×50 mm^2, depending on the manual movement speed. The obtained images were processed, segmented and transformed to the global coordinate system by the embedded camera algorithms. The homography calibration matrix was obtained with a south-shape target and the uncertainty of calibration was experimentally proved not to exceed 0.01 mm. The scanning results, in the form of a cloud of points, were sent via the Ethernet interface to a computer for further processing. No filter was used here to analyse the surface topography data. In order to avoid the error of placing different samples under the scanner the data was levelled [52]. The data is saved in "*.csv" format. The final result of the scanning is a 3D isometric view of the examined surface. The isometric view is then analysed in external software to acquire the values of the 3D roughness parameters.

The main advantages of the newly designed 3D scanner are the possibility to perform non-contact surface analysis, speed, accuracy of measurement sufficient enough to analyse the concrete surface morphology and also mobility. It is worth noting that the weight of the scanner is less than 5 kg. Additionally, the size of the tested area is equal to 50 mm × 50 mm, as is the case in the analysis of the pull-off adhesion of layers in multi-layered concrete elements.

The 3D scanner's main disadvantage is the necessity of levelling the device at each subsequent change of research site. Also, as mentioned in [52], uncertainty of the 3D scanner depends mainly on the accuracy of the light profile calculation and on the calibration of the system. Since the methods offer subpixel accuracy, the optical parameters of the lenses (distortions, aberrations and MTF) must be taken into account. Moreover, the imaging of the light profile strongly depends on the optical properties of the surface (scattering, absorptivity, normal surface variations) [52].

4. Description of conducted research

Three sample concrete elements with dimensions of 1500 × 750 mm^2 and a thickness of 40 mm each were subjected to analyses (Fig. 3). The concretes, from which the elements were

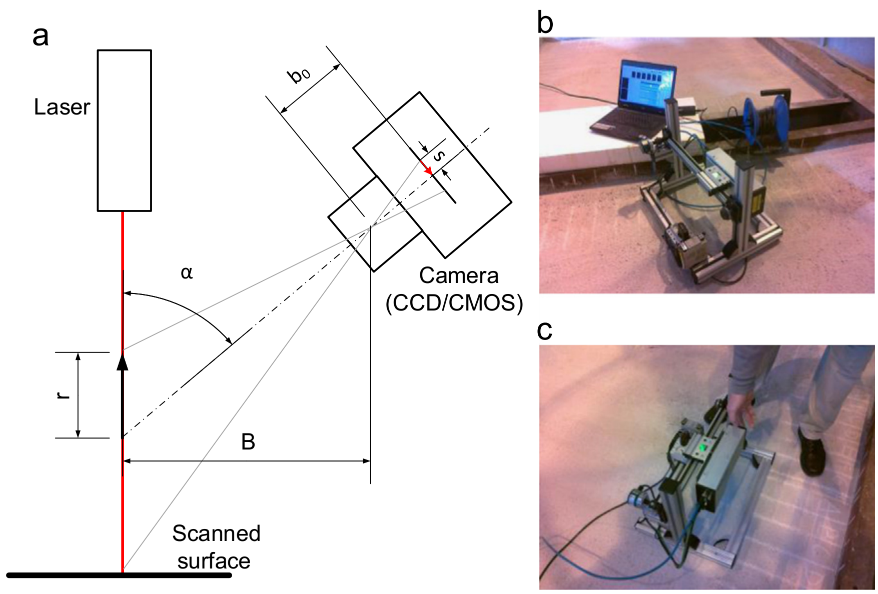

Fig. 2. View of: (a) scheme of adopted laser triangulation system, (b) test setup for investigating the existing concrete substrate surface roughness by 3D laser scanning using a laser triangulation scanner, and (c) surface scanning process [52].

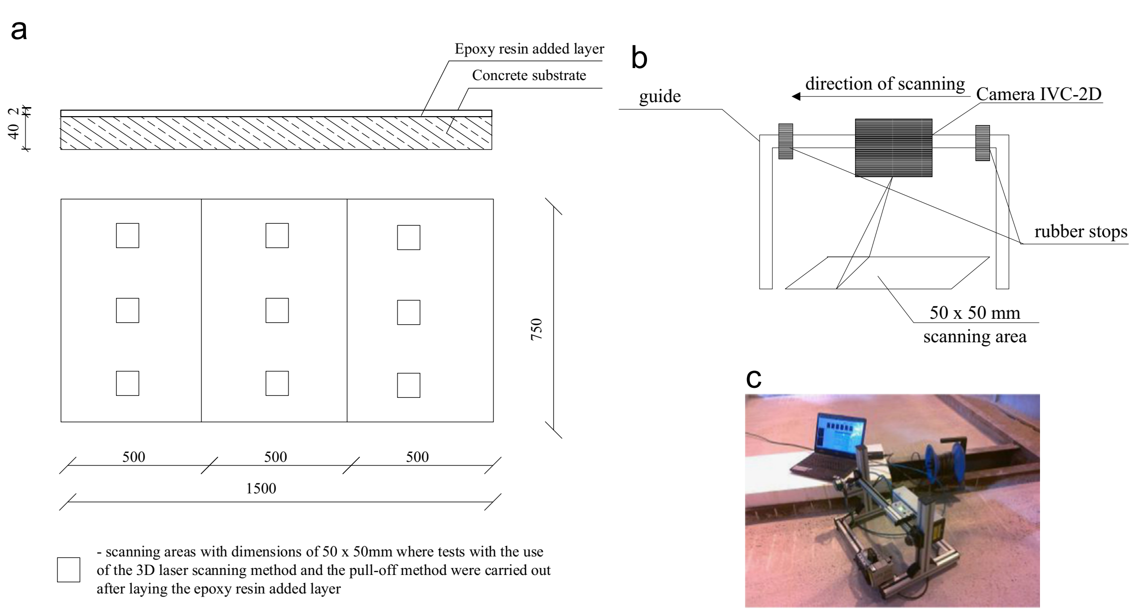

Fig. 3. Tested element with distributed scanning areas (a), the diagram (b), and the view (c) of the test stand for analysing the surface morphology with the use of a newly constructed 3D scanner.

made, differed in terms of maximum grain size of used quartz aggregate (Table 3).

The concretes were cured naturally at an air relative humidity of 60% (±5%) and an air temperature of +20 °C (±3 °C). For the first seven days the concretes were kept under PVC sheeting. Table 4 shows the average values of the selected physical and mechanical parameters of these concretes which were determined after 28 days.

In order to diversify the surface morphology of the tested elements, each of them was divided into three equal parts with dimensions equal to 500 mm × 750 mm as shown in Fig. 3. The surface of each piece was treated in the way presented in Fig. 4. Based on the literature survey, three ways have been selected. The first concrete surface (raw) was not specially treated and this in practice is the most popular method (patch grabbing). The second surface (ground) was treated using a hand-held angle grinder with an abrasive disc and dust removal to reduce roughness. The third one was shotblasted by using a lightweight shotblasting system with dust removal with a buckshot diameter of 6 mm to increase the surface roughness.

A total of nine model surfaces, which differ due to their morphology, were obtained and analysed with the use of the constructed 3D scanner.

Measuring areas of 50 × 50 mm^2 were assessed. Areas of this size are subjected to tests with the use of the pull-off method in construction practice in order to assess the interlayer pull-off adhesion.

Subsequently, after completing the surface roughness analyses of these surfaces, an epoxy resin added layer with a thickness of 2 mm was put on them. The added layer was produced using commercially available epoxy resin StoPox BB OS [57]. The two-component composite formed on the basis of epoxy resin cured with phthalic anhydride with a declared density from 1.41 to 1.49 g/cm^3 and viscosity between 1400 and 2300 mPa s during mixing. A compressive strength equal to 60 MPa was declared with tensile strength equal to 30 Mpa and Young modulus equal to 1450 MPa. Before the application of epoxy resin the concrete substrate was dry, load bearing and free of homogeneous or foreign substances with a separating effect. Measured surface tensile strength f_{hs} of concrete substrates determined by pull-off method was minimum 1.5 MPa. Similarly to the concretes, the resin cured naturally at an air relative humidity of 60% (±5%) and an air temperature of +20 °C (±3 °C).

After 28 days, tests of the pull-off adhesion of the epoxy resin added layer and concrete substrate were conducted with the use of the pull-off method (Fig. 5). They were made in the same

Table 3
Composition of the concrete mixes.

No. of element [dimensionless]	Sand 0–2 mm [kg/m^3]	Crushed quartz aggregate 2–4 mm [kg/m^3]	Crushed quartz aggregate 2–8 mm [kg/m^3]	Maximum size of grain equal to D_{max} [mm]	Superplasticizer + Polypropylene fibres [kg/m^3]	Water [l]	CEM V/A(S-V) 32,5R LH [kg/m^3]
1	1790	–	–	2	2.20	140	280
2	1074	716	–	4	2.20	140	280
3	1074	–	716	8	2.20	140	280

Table 4
Average values of the physical and mechanical parameters of concretes after 28 days.

No of element [dimensionless]	Porosity p [%]	Absorptivity N_w [%]	Relative humidity w [%]	Compressive strength f_{cm} [MPa]
1	26.90	10.27	4.78	12.81
2	24.36	9.94	3.96	14.16
3	23.21	8.68	4.05	17.60

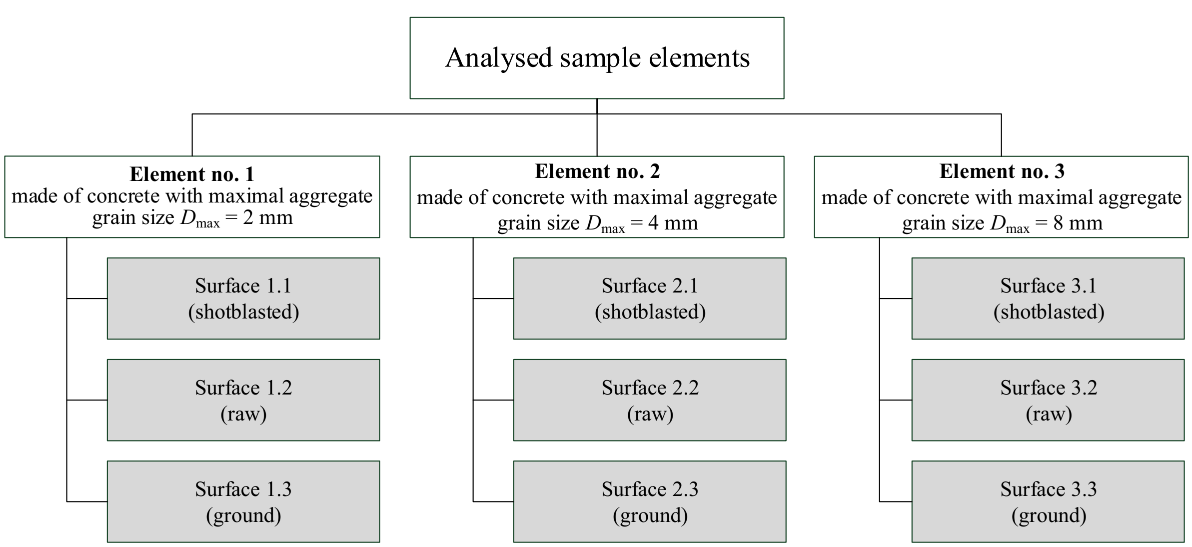

Fig. 4. Designation of the surfaces of tested elements with consideration of how they are treated.

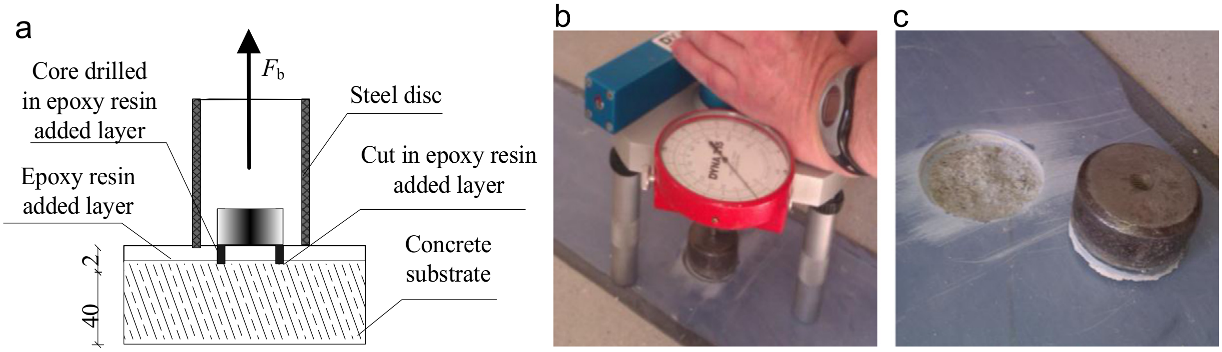

Fig. 5. View of: (a) the test stand for testing the pull-off adhesion with the use of the pull-off method, (b) performing tests, and (c) the top layer after the test.

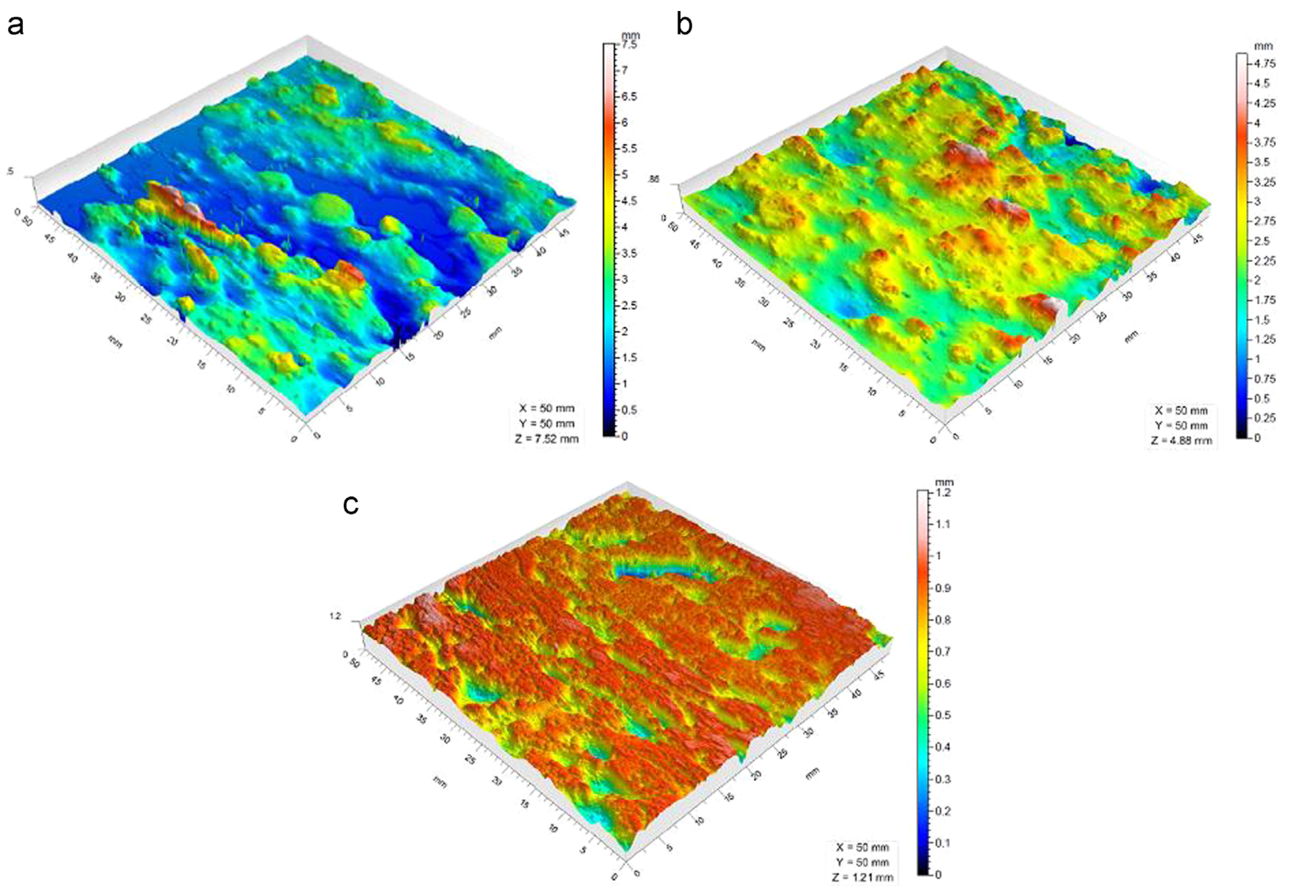

Fig. 6. Sample 3D isometric views of surfaces: 1.1 (a), 1.2 (b), and 1.3 (c).

measuring areas located on the surfaces of the analysed elements, in which surface morphology analysis was carried out with the newly designed 3D scanner. Tests with the use of the pull-off method include the execution of drilling holes with diamond core drill with a diameter of 50 mm at an angle of 90° (± 1°) in the top layer, bonding of steel discs and then finally pulling them off the base surface, with the tension force at a steady load rate of 0.05 MPa/s, with a special actuator with registration of the pull-off force F_b [58]. Load has been applied to the centre of the disc at an angle of 90° (± 1°). Knowing the average size of the diameter D_f of the pulled off steel disc, the pull-off adhesion value f_b is obtained according to [59] from the formula (2):

$$f_b = \frac{4 \cdot F_b}{\pi \cdot {D_f}^2} \tag{2}$$

5. Results and discussion

Fig. 6 shows the exemplary 3D isometric views of surfaces 1.1, 1.2 and 1.3, which were obtained on the basis of research carried out with the use of the constructed 3D scanner.

For each of the 9 analysed surfaces, the average values of 6 height parameters were designated as follows: arithmetical mean height (*Sa*), the root-mean square height (*Sq*), skewness (*Ssk*), kurtosis of the 3D surface texture height distribution (*Sku*), the maximum peak height (*Sp*), the maximum pit height (*Sv*) and also the pull-off adhesion f_b was determined with the use of the pull-off method. The *Sz* parameter was omitted due to the fact that its value according to equation (1) is the difference of *Sp* and *Sv*.

Tables 5–7 show the test results in the form of selected statistical characteristics of the obtained results.

Table 5
Selected statistical characteristics of the parameters obtained in the measurement areas located on the surface of element 1.

Parameter symbol	Name and value of characteristic								
	1.1			1.2			1.3		
	Average	Standard deviation	Variation coefficient [%]	Average	Standard deviation	Variation coefficient [%]	Average	Standard deviation	Variation coefficient [%]
Height parameters									
Sa [mm]	0.121	0.023	19.2	0.123	0.010	7.9	0.134	0.023	16.9
Sq [mm]	0.149	0.026	17.6	0.150	0.012	8.1	0.161	0.026	16.1
Ssk [dimensionless]	−0.178	0.113	−63.1	0.144	0.142	98.6	0.182	0.051	27.8
Sku [dimensionless]	2.870	0.335	11.7	2.563	0.212	8.3	2.395	0.124	5.2
Sp [mm]	0.516	0.021	4.0	0.580	0.037	6.4	0.535	0.048	8.9
Sv [mm]	0.732	0.108	14.7	0.549	0.098	17.8	0.601	0.120	20.0
Pull-off adhesion									
f_b [MPa]	1.562	0.154	9.9	1.621	0.182	11.2	1.617	0.220	13.6

Table 6
Selected statistical characteristics of the parameters obtained in the measurement areas located on the surface of element 2.

Parameter symbol	Name and value of characteristic								
	2.1			2.2			2.3		
	Average	Standard deviation	Variation coefficient [%]	Average	Standard deviation	Variation coefficient [%]	Average	Standard deviation	Variation coefficient [%]
Height parameters									
Sa [mm]	0.175	0.013	7.2	0.157	0.006	3.8	0.151	0.042	27.8
Sq [mm]	0.212	0.015	7.1	0.193	0.009	4.7	0.180	0.044	24.4
Ssk [dimensionless]	0.10	0.01	12.6	0.08	0.16	195.1	−0.09	0.21	-245.7
Sku [dimensionless]	2.480	0.010	0.4	2.635	0.125	4.7	2.740	0.760	27.7
Sp [mm]	0.689	0.077	11.2	0.613	0.029	4.8	0.563	0.061	10.9
Sv [mm]	0.740	0.064	8.6	0.714	0.057	8.1	0.726	0.133	18.3
Pull-off adhesion									
f_b [MPa]	1.726	0.006	0.3	1.755	0.125	7.1	2.343	0.153	6.530

Table 7
Selected statistical characteristics of the parameters obtained in the measurement areas located on the surface of element 3.

Parameter symbol	Name and value of characteristic								
	3.1			3.2			3.3		
	Average	Standard deviation	Variation coefficient [%]	Average	Standard deviation	Variation coefficient [%]	Average	Standard deviation	Variation coefficient [%]
Height parameters									
Sa [mm]	0.201	0.018	9.2	0.117	0.023	19.8	0.139	0.006	4.3
Sq [mm]	0.242	0.017	6.8	0.147	0.027	18.4	0.168	0.007	4.5
Ssk [dimensionless]	0.15	0.11	71.8	−0.02	0.12	595.6	0.40	0.07	18.2
Sku [dimensionless]	2.415	0.235	9.7	3.190	0.400	12.5	3.245	0.725	22.3
Sp [mm]	0.778	0.032	4.2	0.625	0.002	0.3	1.178	0.303	25.7
Sv [mm]	0.815	0.043	5.2	0.655	0.027	4.1	0.562	0.056	9.9
Pull-off adhesion									
f_b [MPa]	2.063	0.229	11.1	2.343	0.407	17.4	2.979	0.382	12.8

It is visible from Tables 5–7 that the lowest values of pull-off adhesion were obtained for the shotblasted surface. For the concretes with a maximum aggregate size of 2 mm, in order to increase the pull-off adhesion it is better to leave the surface without special treatment, and for the concretes with a maximum aggregate size of 4 and 8 mm it is better to use grinding in order to increase the pull-off adhesion.

Fig. 7 presents the course of average values of several of the 3D roughness parameters which were obtained during research in relation to the maximum size of aggregate grain in concrete D_{max} and the way of treating the surface of the analysed element.

When analysing the results of research presented in Fig. 7 it can be seen that the values of parameters *Sa* and *Sq* have a similar course. For the surface of the element made of concrete with a

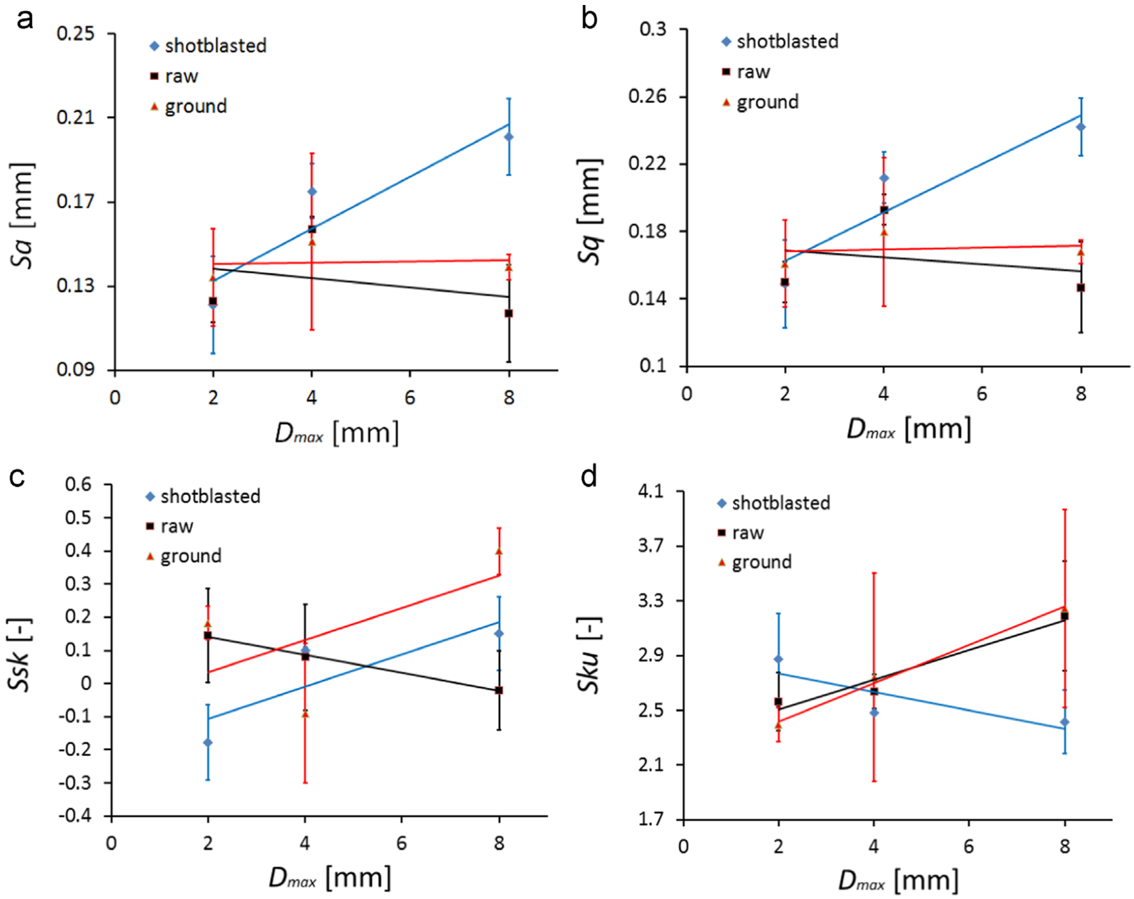

Fig. 7. The course of average values of *Sa* (a), *Sq* (b), *Ssk* (c) and *Sku* (d) parameters in relation to the maximum size of aggregate grain in concrete D_{max} and the method of surface treatment.

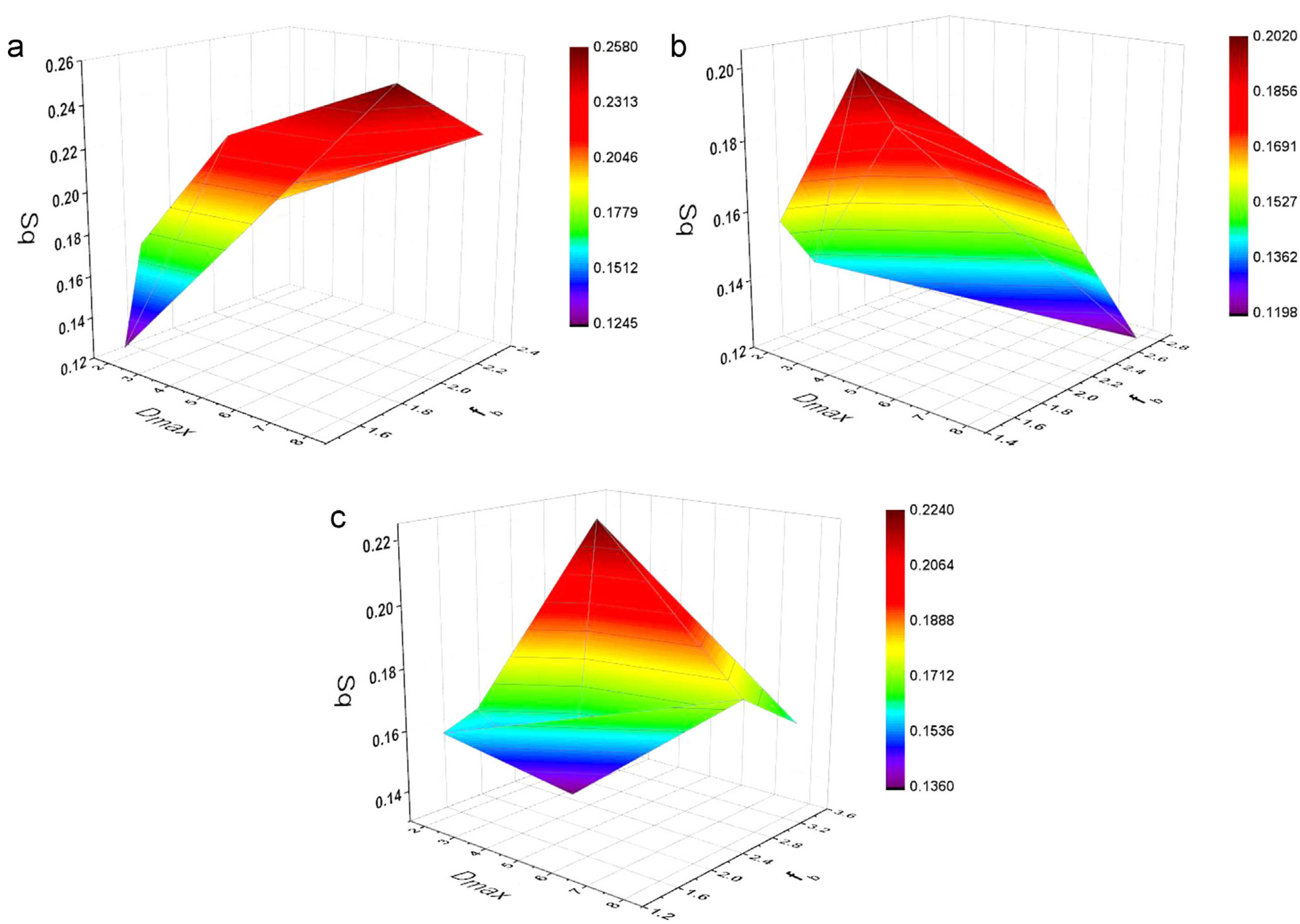

Fig. 8. The formation of the average values of roughness parameter *Sq* in relation to the maximum aggregate grain size in concrete D_{max} and the method of the surface

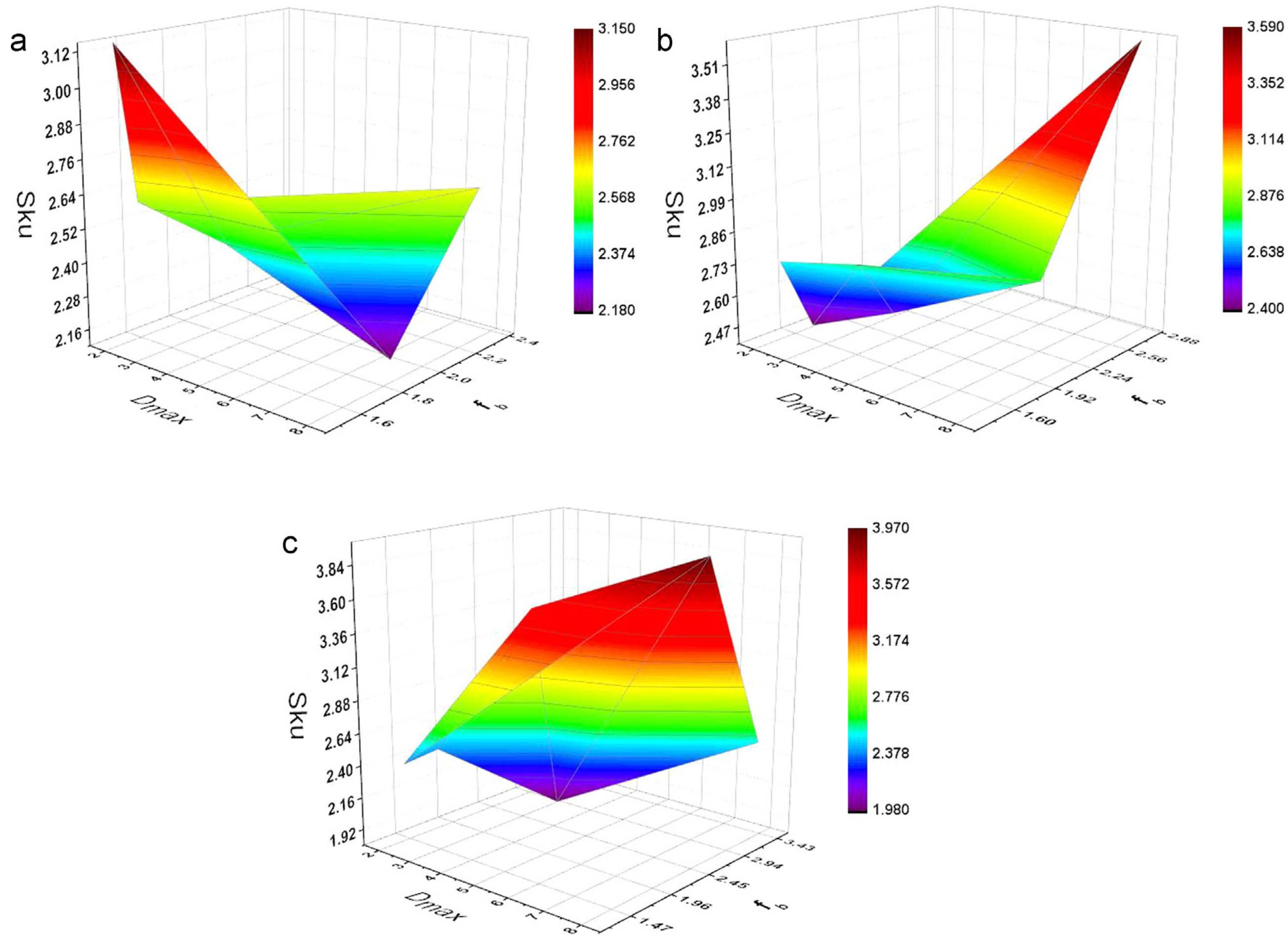

Fig. 9. The formation of the average values of roughness parameter *Sku* in relation to the maximum aggregate grain size in concrete D_{max} and the method of the surface treatment, and also in conjunction with the pull-off adhesion f_b of the epoxy resin added layer: (a) the shotblasted surface, (b) the raw surface. and (c) the ground surface.

maximum aggregate grain size D_{max}=2 mm the values of *Sa* and *Sq* are similar to each other regardless of the method of the surface treatment. With an increase of the maximum aggregate grain size in concrete D_{max}, the values of *Sa* and *Sq* clearly grow for the shotblasted surface.

Regarding parameter *Ssk*, it can be noted that with an increase of the maximum aggregate grain size in concrete D_{max}, its value increases for the shotblasted surface from −0.192 for D_{max}=2 mm to 0.384 for D_{max}=8 mm. In turn, *Ssk* decreases for the ground surface from 0.120 for D_{max}=2 mm to about 0 for D_{max}=8 mm. Thus, *Ssk* has positive values for all cases except for the shotblasted surface of concrete with an aggregate grain size of up to 2 mm and for the ground surface of up to 4 mm respectively. It should be recalled that the symbol *Ssk* defines the majority of peaks ($Ssk>0$) or valleys ($Ssk<0$) on a surface.

In the case of parameter *Sku*, its values clearly grow for the ground surface, and decrease for the shotblasted surface with an increase of maximum aggregate grain size in concrete D_{max}. This parameter only has a value in excess of 3 for the ground surface for D_{max}=8 mm. The obtained results also show that surface treatment by shotblasting causes a decrease in the value of the *Sku* parameter below 3, which may indicate a low probability of defect occurrence and their regular distribution on the analysed surface.

In turn, Figs. 8–10 show the exemplary courses of the average values of the roughness parameters *Sq*, *Sku* and *Ssk* in relation to the maximum aggregate grain size in concrete and the method of the surface treatment of the analysed element in conjunction with the pull-off adhesion value f_b of the polymer top layer to the tested concrete surface. The analysis did not include the *Sa* parameter because it has a similar course to *Sq*.

Fig. 8 shows that for the shotblasted surface (Fig. 8a) with increasing values of *Sq* parameter and aggregate grain size in concrete D_{max}, the value of the pull-off adhesion f_b of the epoxy resin added layer laid on the tested surface grows. For the ground surface (Fig. 8b), for which the maximum values of the pull-off adhesion f_b were obtained for the surface of the element made of concrete with a maximum aggregate grain size D_{max}=8 mm, the values of the *Sq* parameter are the lowest.

However, Fig. 9 shows that with an increase of the value of *Sku* parameter and the aggregate grain size in concrete D_{max}, the value of the pull-off adhesion f_b grows for the ground surface (Fig. 9a) and the raw surface (Fig. 9b), while shotblasting causes a decrease in the value of the *Sku* parameter and a simultaneous increase in the value of the pull-off adhesion f_b.

In turn, Fig. 10 shows that for the shotblasted surface with increasing *Ssk* parameter values and aggregate grain size in concrete D_{max}, the value of the pull-off adhesion f_b for the ground surface grows. The surface of the element made of concrete with a maximum aggregate grain size D_{max}=8 mm has *Ssk* parameter values above 0 and also the highest obtained values of the pull-off adhesion f_b.

In order to check the correlation between the height parameters of the concrete substrate and their pull-off adhesion to epoxy resin, their correlation with the linear correlation coefficient and Spearman's rank correlation coefficient was determined for all the applied methods of the surface treatment (Table 8).

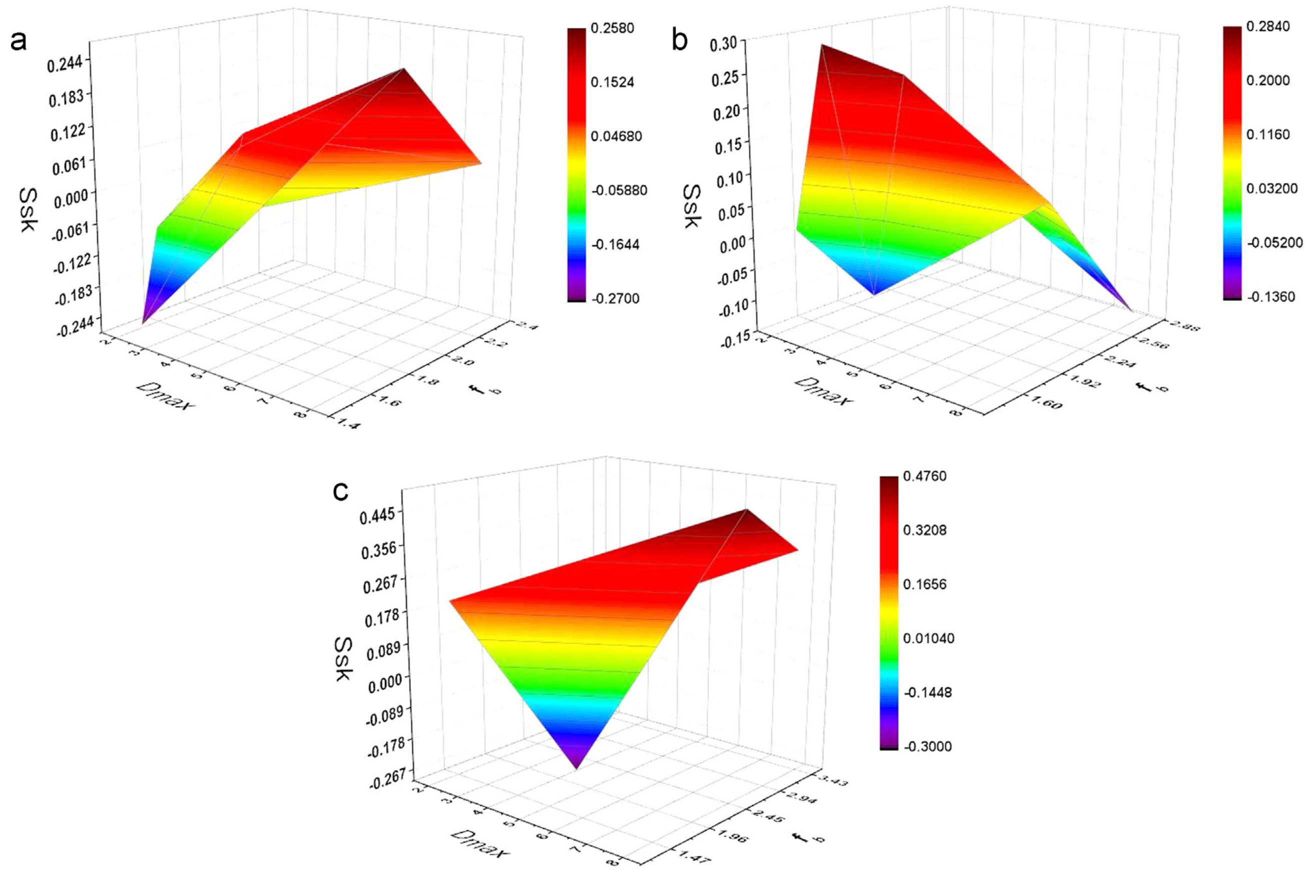

Fig. 10. The formation of the average values of roughness parameter *Ssk* in relation to the maximum aggregate grain size in concrete D_{max} and the method of the surface treatment, and also in conjunction with the pull-off adhesion f_b of the epoxy resin added layer: (a) the shotblasted surface, (b) the raw surface, and (c) the ground surface.

Table 8
Calculated values of Spearman's rank correlation coefficient ρ_s and linear correlation coefficients *R*.

Parameter name	Pull-off adhesion f_b between concrete substrate and epoxy resin added layer	
	Spearman's rank correlation coefficient ρ_s	Linear correlation coefficients *R*
Sa [mm]	0.21	0.01
Sq [mm]	0.21	0.01
Ssk [dimensionless]	0.18	0.42
Sku [dimensionless]	0.52	0.72
Sp [mm]	0.69	0.79
Sv [mm]	0.08	0.19

It can be seen from Table 8 that parameters *Sku* and *Sp* are characterized by the highest linear correlation coefficients *R*, *of* 0.72 and 0.79 respectively, and that Spearman's rank correlation coefficient ρ_s is in a range of 0.4–1 for parameters *Sku* and *Sp*, assuming the highest value (0.69) in the case of parameter *Sp*.

6. Summary

It was found that with an increase of maximum aggregate grain size in concrete D_{max}, the values of *Sa*, *Sq* and *Ssk* parameters for the shotblasted surface also increase, while the value of the *Sku* parameter grows for ground and raw surfaces and decreases for the shotblasted surface.

For the tested concretes with a maximum aggregate size of 2 mm and in the case of pull-off adhesion at the concrete substrate/apoxy resin interface, it is better to finish the surface by patch grabbing in order to obtain a raw surface without special surface treatment. For the concretes with a maximum aggregate size of 4 and 8 mm the use of grinding is suggested in order to increase the pull-off adhesion between low-strength concrete substrate and epoxy resin.

It was also found that there is a relation between the values of height parameters *Sq*, *Sku*, and *Ssk* which describe the morphology of the tested concrete surfaces, and the pull-off adhesion of the epoxy resin added layer and these surfaces. Thus, with increasing values of parameters *Sq* and *Ssk* and an increase of the aggregate grain size in concrete D_{max}, the value of the pull-off adhesion f_b of the epoxy resin added layer to the shotblasted surface grows. However, with an increase of the value of the *Sku* parameter and the aggregate grain size in concrete D_{max}, the value of the pull-off adhesion f_b of the epoxy resin added layer to ground and raw surfaces increases.

The highest values of linear correlation coefficient *R*, amounting to 0.7, and the values of Spearman's rank correlation coefficient have been obtained for two parameters: the kursosis (*Sku*) and the maximum height of peaks (*Sp*). However, the values are too low to definitely conclude that it is possible to determine the pull-off adhesion f_b of the epoxy resin added layer solely on the basis of the existing concrete substrate layer surface morphology examinations.

Acknowledgements

The research presented in the article have been supported by the Foundation for Polish Science (FNP).

Special acknowledgements to Prof. Thomas G. Mathia from Laboratoire de Tribologie et Dynamique des Systemes (Ecole Centrale de Lyon) for valuable exchange of opinions related to concrete surface morphology.

The authors are also grateful to Zaremba Posadzki sp. z o.o. from Słotwina 65 58-100 Świdnica for sharing their recipe for the existing concrete substrate.

References

[1] Mikami T, Kang Y, Choi S. Judging indices for evaluating the exfoliation of synthetic resin floorings using the impact acoustics method. Constr Build Mater 2015;95:345–54.
[2] Garbacz A, Courard L, Bissonnette B. A surface engineering approach applicable to concrete repair engineering. Bull Pol Acad Sci: Tech Sci 2013;61(1):73–84.
[3] Garbacz A. Application of stress based NDT methods for concrete repair bond quality control. Bull Pol Acad Sci: Tech Sci 2015;63(1):77–85.
[4] Whitehouse D. Handbook of surface metrology. Bristol: Institute of Physics Publishing; 1994.
[5] ISO/R 468 Surface roughness—Parameters, their values and general rules for specifying surfaces: International Organization for Standardization, Geneva; 1966
[6] ISO 4287 Geometrical product specifications-surface texture: profile method
[7] Erdem S, Dawson A, Thom N. Impact load-induced micro-structural damage and microstructure associated mechanical response of concrete made with different surface roughness and porosity aggregates. Cem Concr Res 2012;42:291–305.
[8] Courard L. Evaluation of thermodynamic properties of concrete substrates and cement slurries modified by admixtures. Mater Struct 2002;35(3):149–55.
[9] Courard L. Adhesion of repair systems to concrete: influence of interfacial topography and transport phenomena. Mag Concr Res 2005;57(5):273–82.
[10] Courard L, Nélis M. Surface analysis of mineral substrates for repair works: roughness evaluation by profilometry and surfometry analysis. Mag Concr Res 2003;55(4):355–66.
[11] Courard L. Parametric study for the creation of the interface between concrete and repair products. Mater Struct 2000;33(1):65–72.
[12] Franck A, De Belie N. Concrete floor-bovine claw contact pressures related to floor roughness and deformation of the claw. J Dairy Sci 2006;89(8):2952–64.
[13] Santos P, Julio E. Correlation between concrete-to-concrete bond strength and the roughness of the substrate surface. Constr Build Mater 2007;21(8):1688–95.
[14] Santos P, Julio E. Development of a laser roughness analyser to predict in situ the bond strength of concrete-to-concrete interfaces. Mag Concr Res 2008;60(5):329–37.
[15] Siewczyńska M. Method for determining the parameters of surface roughness by usage of a 3D scanner. Arch Civ Mech Eng 2012;12(1):83–9.
[16] Garbacz A, Courard L, Kostana K. Characterization of concrete surface roughness and its relation to adhesion in repair systems. Mater Charact 2006;56(4–5):281–9.
[17] Maerz H, Chepur P, Myers J, Linz J. Concrete roughness characterization using laser profilometry for fiber-reinforced polymer sheet application. In: Proceedings of the transportation research board 80th annual meeting. Washington; January 7–11, 2001.
[18] Garbacz A, Górka M, Courard L. Effect of concrete surface treatment on adhesion in repair systems. Mag Concr Res 2005;57:49–60.
[19] Silfwerbrand J, Paulsson J. Better bonding of bridge deck overlays. Concr Int 1998;10:56–61.
[20] Courard L, Schwall D, Garbacz A, Piotrowski T. Effect of concrete substrate texture on the adhesion properties of PCC repair mortar. Proc Inter Symp Polym Concr ISPIC 2006:99–110.
[21] Júlio E, Branco F, Silva V, Lourenço J. Influence of added concrete compressive strength on adhesion to an existing concrete substrate. Build Environ 2006;41(12):1934–9.
[22] Moghtadaei R, Mohammadi M, Samani N, Mousavi S. The impact of surface preparation on the bond strength of repaired concrete by metakaolin containing concrete. Constr Build Mater 2015;80:76–83.
[23] Julio E, Branco F, Silva V. Concrete-to-concrete bond strength. Influence of the roughness of the substrate surface. Constr Build Mater 2004;18(9):675–81.
[24] Júlio E, Branco F, Silva V. Concrete-to-concrete bond strength: influence of an epoxy-based bonding agent on a roughened substrate surface. Mag Concr Res 2005;57(8):463–8.
[25] Santos P, Júlio E. Factors affecting bond between new and old concrete. ACI Mater J 2011;108(4):449–56.
[26] Courard L, Piotrowski T, Garbacz A. Near-to-surface properties affecting bond strength in concrete repair. Cem Concr Compos 2014;46:73–80.
[27] Courard L, Schwall D, Garbacz A, Piotrowski T. Effect of concrete substrate texture on the adhesion properties of PCC repair mortar. In: Aguiar JB, Jalali S, Camões A, Ferreira RM, editors. Proceedings ISPIC 2006 international symposium polymers in concrete. Guimarães, Oficinas Gráficas de Barbosa & Xavier, Lda, Braga, Portugal; 2006: p. 99–110.
[28] Stout K, Sullivan P, Dong W, Mainsah E, Luo N, Mathia T, Zahouani H. The development of methods for the characterisation of roughness in three dimensions. Birmingham: University of Birmingham Edgbaston; 1993.
[29] ISO 25178: Geometric product specifications (GPS)-surface texture: areal
[30] CEB-FIP Model Code 2010. Comité Euro-International du Béton Secretariat Permanent. Case Postale 88, CH-1015 Lausanne, Switzerland; 2010.
[31] Adams R, Drinkwater B. Nondestructive testing of adhesively-bonded joints. NDT E Int 1997;30(2):93–8.
[32] Sezen H, Fisco N. Evaluation and comparison of surface macrotexture and friction measurement methods. J Civ Eng Manag 2013;19(3):387–99.
[33] Santos P, Júlio E. A state-of-the-art review on roughness quantification methods for concrete surfaces. Constr Build Mater 2013;38:912–23.
[34] Santos P, Júlio E. Effect of filtering on texture assessment of concrete surfaces. ACI Mater J 2010;107(1):31–6.
[35] Mathia T, Pawlus P, Wieczorowski M. Recent trends in surface metrology. Wear 2011;271:494–508.
[36] Santos P, Júlio E. Comparison of methods for texture assessment of concrete surfaces. ACI Mater J 2010;107(5):433–40.
[37] Niemczewska-Wójcik M, Mathia T, Wójcik A. Measurement techniques used for analysis of the geometric structure of machined surfaces. Manag Prod Eng Rev 2014;5(2):27–32.
[38] Blateyron F. New 3D parameters and filtration techniques for surface metrology; 2007. ⟨www.qualitymag.com/articles/85037⟩.
[39] Ali S. Advanced nanomeasuring techniques for surface characterization. ISRN Opt 2012 Article ID 859353.
[40] ⟨http://www.zeiss.com/⟩.
[41] Ourahmoune R, Salvia M, Mathia T, Berthel B, Fouvry S, Mesrati N. Effect of sandblasting substrate treatment on single lap shear strength of adhesively bonded PEEK and its composites. In: Proceedigns of the 18th international conference on composite materials. Jeju Island, Korea; 2011.
[42] Kurganskaya I, Luttge A, Barron A. The application of VSI (Vertical Scanning Interferometry) to the study of crystal surface processes. ⟨http://cnx.org/content/m22326/1.4/⟩.
[43] McMullan D. Scanning electron microscopy 1928–1965. Scanning 2006;17(3):175–85.
[44] Ficker T, Martišek D. Three-dimensional reconstructions of solid surfaces using conventional microscopes. Scanning 2015. http://dx.doi.org/10.1002/sca.21238.
[45] Tayeh B, Bakar B, Johari M, Voo Y. Mechanical and permeability properties of the interface between normal concrete substrate and ultra high performance fibre concrete overlay. Constr Build Mater 2012;36:538–48.
[46] Tayeh B, Bakar B, Johari M, Ratnam M. The relationship between substrate roughness parameters and bond strength of ultra high-performance fibre concrete. J Adhes Sci Technol 2013;27(16):1790–810.
[47] Majchrowski R, Grzelka M, Wieczorowski M, Sadowski L, Gapiński B. Large area concrete surface topography measurements using optical 3D scanner. Metrol Meas Syst 2015:4 in press.
[48] Werner S, Neumann I, Thienel K, Heunecke O. A fractal-based approach for the determination of concrete surfaces using laser scanning techniques: a comparison of two different measuring systems. Mater Struct 2013;46(1-2):245–54.
[49] Czarnecki S, Hoła J, Sadowski Ł. A non-destructive method of investigating the morphology of concrete surfaces by means of newly designed 3D scanner. In: Proceedings of the 11th European conference on non-destructive testing. Prague, Czech Republic; 2014.
[50] Niemczewska-Wójcik M, Mańkowska-Snopczyńska A, Piekoszewski W. The investigation of wear tracks with the use of noncontact measurement methods. Arch Civ Mech Eng 2013;13(2):158–67.
[51] Ourahmoune R, Salvia M, Mathia T, Mesrati N. Surface morphology and wettability of sandblasted PEEK and its composites. Scanning 2014;36(1):64–75.
[52] Hoła J, Sadowski Ł, Reiner J, Stach S. Usefulness of 3D surface roughness parameters for nondestructive evaluation of pull-off adhesion of concrete layers. Constr Build Mater 2015;84:111–20.
[53] Sadowski L. Application of three-dimensional optical laser triangulation method for concrete surface morphology measurement. Indian J Eng Mater Sci 2014;21:692–700.
[54] Sioma A. The estimation of resolution in 3D range image system. In: Proceedings of the 14th international Carpathian control conference (ICCC); 2013: p. 346–9.
[55] Reiner J, Stankiewicz M. Evaluation of the predictive segmentation algorithm for the laser triangulation method. Metrol Meas Syst 2011;18(4):667–78.
[56] Pernkopf F, O'Leary P. Image acquisition techniques for automatic visual inspection of metallic surfaces. NDT E Int 2003;36(8):609–17.
[57] ⟨http://www.sto.pl/129718_PL–StoPox_BB_OS_PL.pdf⟩.
[58] PN-EN 12504-3: 2005. Analysis of concrete in constructions. Part 3: Determination of the pull-out force. PKN, Warsaw; 2006
[59] ASTM D7234–05. Standard test method for pull-off adhesion strength of coatings on concrete using portable pull-off adhesion testers; 2005